Mediterranean Archaeology and Archaeometry, Vol. 16, No 2,(2016), pp. 139-148

DOI:10.5281/zenodo.53072

ROMAN BEDROCK MORTARS: NEW FINDINGS FOR INTERPRETING DATA AT THE ROMAN PINO DEL ORO GOLD MINES (SPAIN)

C. Vázquez-Calvo[1], R. Fort[1], D. Romero[2], A. Beltrán[2] and F. J. Sánchez-Palencia[2]

[1]Instituto de Geociencias (CSIC,UCM), c/ José Antonio Nováis 12, Madrid, Spain
[2]Instituto de Historia. CCHS. CSIC, c/ Albasanz, nº 26-28, Madrid, Spain

Received: 10/12/2015
Accepted: 25/05/2016
Corresponding author: C.Vazquez-Calvo(carmenvazquez@geo.ucm.es)

ABSTRACT

The Pino del Oro gold mines, located in the northwestern Iberian Peninsula and more specifically in the Spanish province of Zamora, form part of the country's Roman Age mining heritage. These mines differ from all the others in the empire in one respect: they are characterised by the presence of quern-like depressions found in the nearby granitic outcrops where miners ground the ore. A series of petrological techniques was used to determine the most appropriate procedure for gathering information that would help clarify the significance of these man-made formations and whether the type of granite was a conditioning factor in the choice of grinding site. An analysis of the results yielded by the techniques deployed to characterise the two types of granite where the bedrock mortars are found showed that ultrasound velocity (Vp) and the hardness index are the two most suitable for futher research. On the grounds of the Vp and hardness fingings, a hypothesis is put forward on how to determine the stage of usability of the bedrock mortars.

KEYWORDS: Roman gold mines, BRM, ultrasound velocity, hardness, petrophysics, north-western Iberian Peninsula.

1. INTRODUCTION

The Pino del Oro gold mines form part of the Iberian Peninsula's Roman Age mining heritage. This complex is located in the north-western part of the peninsula and more specifically in the Spanish province of Zamora (see the site map in Figure 1). Due partly to its remoteness from other gold outcrops (according to the inventory of mineral resources in Castile and Leon, the region to which Zamora belongs, Pino del Oro is an isolated outcrop; Jiménez Benayas et al., 1997), little was known about the complex until archaeological studies were begun in 2006. Operations in the 70-some mining sites in the area have been dated to the Early Roman Empire (first-second centuries AD) (Sánchez-Palencia et al., 2010a).

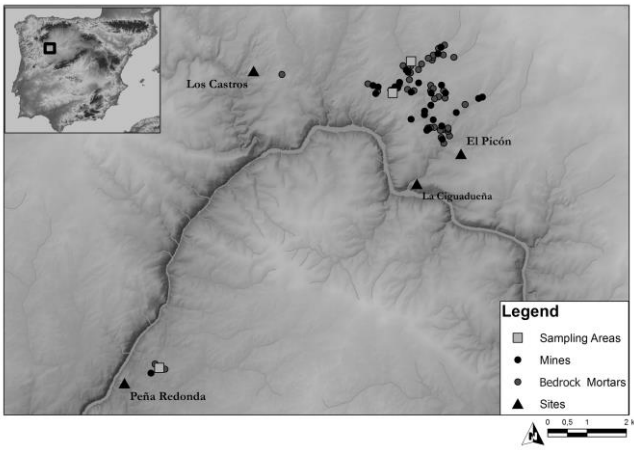

Figure 1. Site map

2. GEOMORPHOLOGICAL AND GEOLOGICAL SETTING

The sites are located in Arribes del Duero, an area exhibiting the smooth reliefs, raised granitic peneplains, and screes and boulders characteristic of granitic landscapes (see Figure 2 for an overview).

Figure 2. Overview of granitic landscape surrounding the Pino del Oro mining complex

The outcrops studied, which comprise two types of granites, are located in the south-eastern corner of the Central Iberian Zone in the Iberian Massif. One is a monzogranitic pluton while the other, the older of the two known as the Ricobayo pluton, is a granodiorite (Quiroga de la Vega et al., 1981, 1982). Both kinds of rocks are described in Vázquez-Calvo et al., (2013). The main constituent minerals in both are quartz, K-feldspar, plagioclase, biotite and muscovite. Their texture differs, however. On the one hand, the K-feldspar content is higher in the monzogranite. And on the other, while "Ricobayo" (oriented NW-SE) exhibits deformities and has a medium grain size and a holocrystalline and allotriomorphic texture, the monzogranitic rock has a coarse grain size with K-feldspar phenocrysts and a holocrystalline and hyphidiomorphic texture (see the pictures of monzogranite and granodiorite in Figure 3).

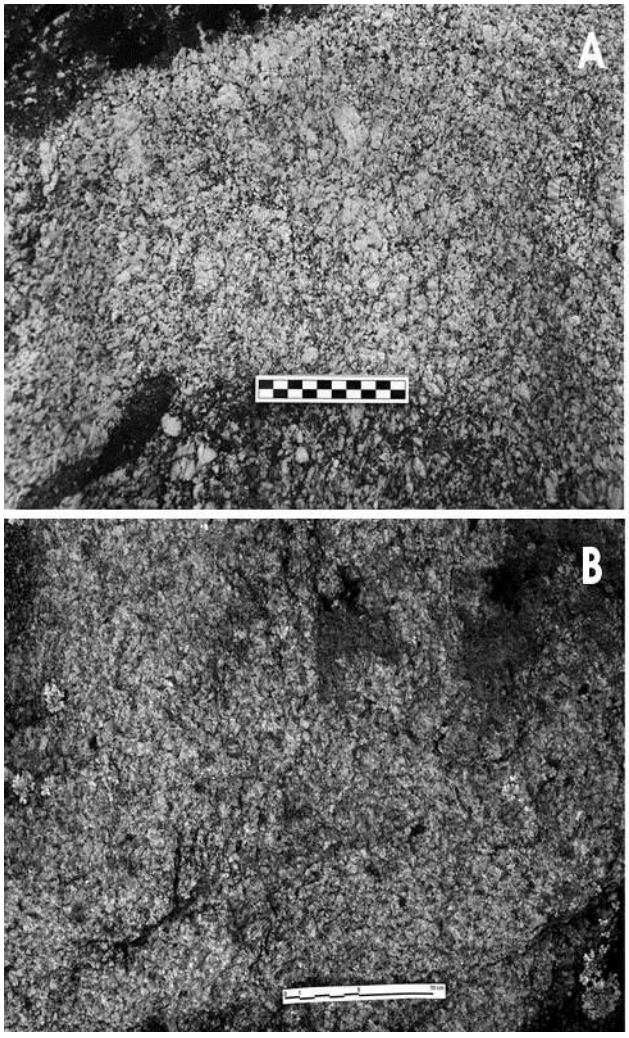

Figure 3. Fresh fractured surfaces. Monzogranite (A) and granodiorite (B)

These granitic outcrops are bound on the north and the south respectively by low and medium-high

grade metamorphic materials with a fairly steep relief. Gold mineralisation runs along a 2 km wide, dextral (N130ºE) brittle-ductile shear zone known as Villadelcampo (González Clavijo et al., 1991). It is associated with two families of quartz veins hosted in the granitic batholiths. These veins, which run essentially N40º to 60ºE and N100ºE (idem) formed during several phases of the Hercynian deformation. Their mineralisation was the result of hydrothermal events in the final stages of development of the Villadelcampo shear zone deformation (Jiménez Benayas et al., 1997: 136). Gold is found in conjunction with the arsenopyrite-pyrite mineralisation identified here, as well as local calcopyrite, sphalerite, magnetite and galena mineralisations. Present in the quartz or breccias that fill the fissures in the host rock, the gold-containing mineralisation forms a subvertical stockwork whose dimensions vary from several meters to a kilometre long and from 5 to 10 metres wide (idem).

3. GOLD MINING: THE HISTORICAL CONTEXT

Variations in the landscape, one of the most important areas of research for understanding gold mining, have served as a source of information on changes in ancient society. The studies conducted to document the Pino del Oro mining area revealed that the gold was extracted with opencast and other open-pit techniques, such as mining 'trenches', a system widely used across the northwestern Iberian Peninsula. Most of the 30-plus mines and 40 grinding identified lie near the village of Pino del Oro, although a few are located in the nearby villages of Castro Alcañices and Villardiegua de la Ribera (see Figure 4 for a large-scale map of the area studied).

Generally speaking, the trenches were small, about 5 to 7 m wide 15 to 20 m long, and up to 7 m deep (see Figure 5 for an example). Some of the mines were larger, however, such as at Corta de los Bueyes, whose exploitation front measured 60 m.

Mining was a very simple affair: the ore was extracted manually with tools such as picks and hammers. According to Pliny the Elder, after extraction the selected ore was crushed, pounded, burnt and ground: "The substance dug out is crushed, washed, fired and pounded to a soft powder" (Plin.NH XXXIII, ch. XXI). In other words, the objective was to convert the mineral into a fine powder.

That this final step in the mining process, grinding, was implemented at Pino del Oro is documented by the existence of depressions in the granite outcrops near the mines (Sánchez-Palencia et al., 2010a). These saddle quern-shaped depressions, called "cazoletas" (literally "small pots") in Spanish, are referred to in this paper as "bedrock mortar" (BRM), borrowing the term applied to similar antrhopogenic depressions left by native Americans.

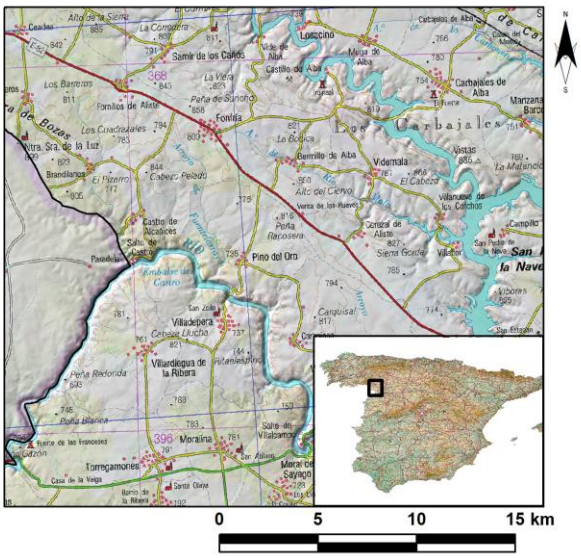

Figure 4. Large-scale map of the area studied

Figure 5. Mining trench dug in the Pino del Oro complex

Such depressions took the place of querns in mortar stones: after the ore was selected, crushed, pounded and burnt, it was ground by rocking a handstone back and forth across the stone outcrop, very likely after first carving a depression in the surface.. Hundreds of bedrock mortars such as depicted in Figure 6 have been identified in the area. They are usually found in groups of over ten or twenty, although clusters of over sixty are not uncommon. Once ground, the powder was washed in nearby streams to separate the gold from other minerals.

Figure 6. Grinding hollows at the Pino del Oro mining complex

Mortar stones have been found at other sites such as the Ptolemaic era gold mines in Egypt, the Laurion silver mines and the Roman gold mines at Tres Minas, Portugal and Dolaucothi, Wales (Burnham and Burnham, 2004; Sánchez-Palencia and Currás Refojos, 2010). In all those cases, however, they were portable tools. The main feature that distinguished the Pino del Oro complex from other mines in the Roman Empire was that the granite outcrops themselves housed the BRMs.

4. OBJECTIVE

The primary aim of the present study was to acquire a better understanding of the role of granite typologies in gold ore grinding and in selecting the working areas. For this reason supplementary data for the outcrop initially studied, 'Pozo Serafín' (Vazquez-Calvo et al., 2013), were acquired using new or modifying existing methods, and two additional outcrops were studied for comparison and to determine the possible influence of the type of granite on the choice of grinding sites. The first criterion for the choice of granite outcrops as BRM sites was obviously the proximity to the extraction operations to minimise processing time by eliminating the need to haul the ore from site to site. Several lines of inquiry might be explored to establish the reasoning underlying what, in light of the consistent presence of BRMs, was presumably a mining strategy systematically implemented in this complex. One is to determine whether the choice of areas was based on rock type; in other words, to establish how accurately ancient miners could distinguish the type of material used for grinding the ore and the extent to which each individual BRM was exploited. To that end, several of these depressions were characterised for their petrophysical and petrographic properties. Studies are presently underway on the time it would have taken to establish BRMs.

5. METHODS

5.1. Sampling

Both types of granites were sampled. Core specimens (4.5 and 5.5 cm in diameter and up to 25 cm long) were extracted from both the BRMs and adjacent rock. The three outcrops selected were: the Pozo Serafín (PS) and Sierpe Tres (ST) granodiorites and the Ribera del Pontón (RB) monzogranite.

5.2. Experimental

As stated in the objectives, the petrophysical and petrographic properties of the granites were determined, both in the laboratory and in situ. Sample petrography and cracking rate were analysed under optical polarised light and fluorescence microscopes.

Petrophysical characterisation included finding surface hardness with a Schmidt hammer (Goudie, 2006; Fort et al., 2013a), and measuring direct (in the laboratory) and indirect (in the field) transmission ultrasound velocity (Vp). The petrological features of stone affect ultrasound velocity: slower velocity denotes greater stone decay (Vazquez-Calvo et al., 2010), provided the samples share the same microstructure. Otherwise, it is an indication of a looser or more porous microstructure. Vp values were also used to find rock anisotropy (Fort et al., 2011). Real and bulk densities, compactness, open porosity, porosity accessible to water and water saturation were determined as recommended by RILEM (1980). Porosity was also assessed using mercury intrusion porosimetry (Onishi and Shimizu, 2005). Finally, roughness, a surface property dependent upon use, petrography and microstructure, was found with a 3D roughness meter (Fort et al., 2013b; Vazquez-Calvo et al., 2012).The instruments used were as follows:

- polarised light microscopy: Olympus BX51 optical microscope (OM) fitted with an Olympus DP12 digital camera, using Olympus DP-Soft (version 3.2) software
-fluorescent microscopy (FM): same microscope and camera as above, fitted with an Olympus U-RFL-T mercury lamp
- surface hardness: original Schmidt Type N Proceq test hammer
- ultrasound velocity (Vp): CNS Electronics Pundit ultrasound velocity gauge; transducer frequency, 54 kHz; contact area, flat and 50 mm in diameter; plasticine-based sealant to secure transducers to the surface in the field
- mercury intrusion porosimetry: Micromeritics Autopore IV 9500 mercury intrusion porosimeter (MIP); pore diameter range, 0.001 to 1 000 μm; pressure range, atmospheric to 60000 psi (228 MPa)
- roughness: TRACEit optical surface (OSR) roughness tester.

6. RESULTS AND DISCUSSION

The mean field ultrasound velocity and the mean field hardness data are given in figure 7. The mean velocity values were observed to be lower and the mean hardness values higher for the BRMs than for the adjacent surfaces. The type of granite also affected the readings, of course. The Vp values for the adjacent surface at Ribera del Pontón were lower than at Pozo Serafín or Sierpe Tres, while the BRM readings were fairly similar in all three, an indication that the value appeared to depend on the depth of the surface of the BRM.

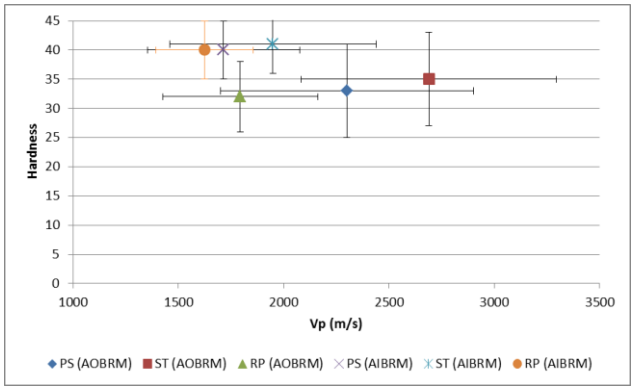

Figure 7. Mean field ultrasound velocity and hardness values. PS: Pozo Serafín, ST: Sierpe Tres, RP: Ribera del Pontón AOBRM: area outside BRM; AIBRM: area inside BRM.

The core specimens were used to determine the variations in the parameter values with depth. Vázquez-Calvo et al. (2013) reported that at the Pozo Serafín outcrop, ultrasound velocity and compactness rose and porosity declined with depth, more visibly from 10 cm inward, confirming that the state of conservation of the rock improved with depth. Open porosity and degree of water saturation were found to decline with depth, as a rule. Hardness also rose with depth inside the BRMs. The mean values for the three outcrops (≈40) did not differ significantly, although the three curves for hardness values measured at points on a line drawn in the lengthwise direction of the depressions were observed to vary (Figure 8). The curves in Figure 8 are representative of the three curve typologies found for the BRMs. The PS 12 curve represents the group of BRMs in which the highest hardness values were found at the centre, where grinding was most intense and hardness was directly related to the depth. RB 11, in turn, represents the group in which hardness was less uniform at the centre of the BRMs, with most values under 40. ST 25 is typical of a third group exhibiting characteristics similar to group RB-11, but with hardness values mostly higher than 40.

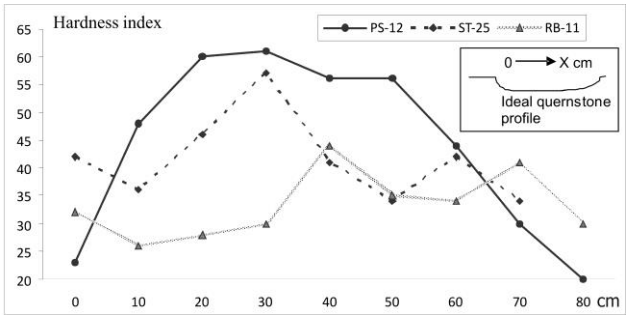

Figure 8. Distribution of hardness index values by lengthwise location of measuring points across several BRMs, showing the differences between the profiles

The microscopic findings for the two kinds of granite showed that the cracks in the monzogranite (outcrop RB) were associated with grain borders (Figure 9).

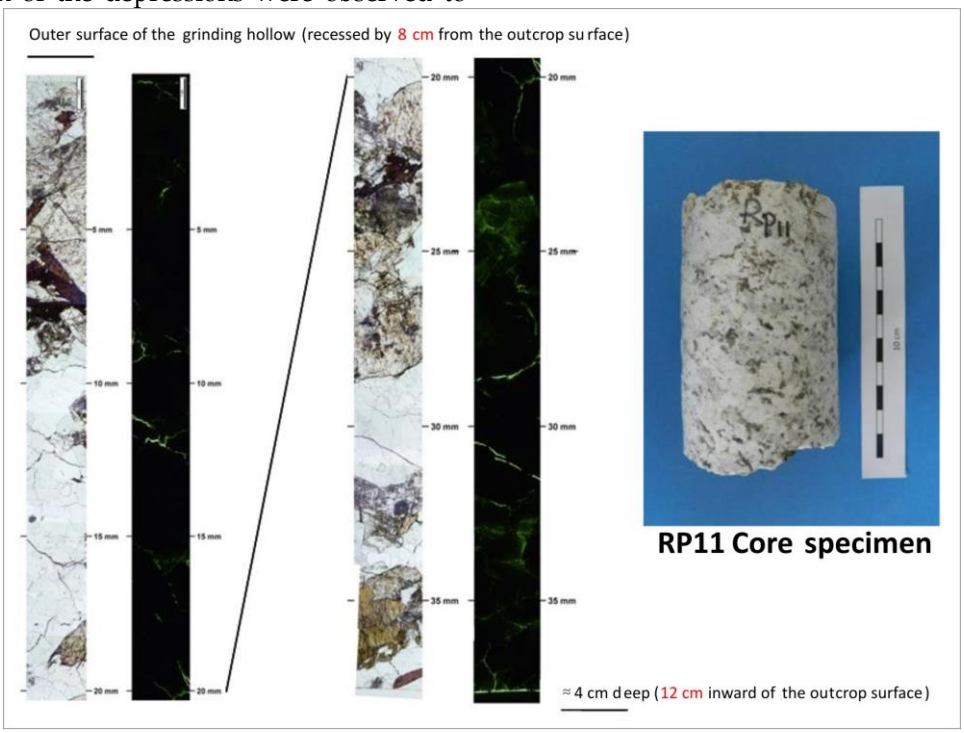

Figure 9. Vertical thin section of core sample RP 11 (Ribera del Pontón): left column, polarised light micrograph; right, fluorescent light micrograph, in which the cracks and pores are more readily visible (each vertical section is a mosaic of 22 microphotographs).

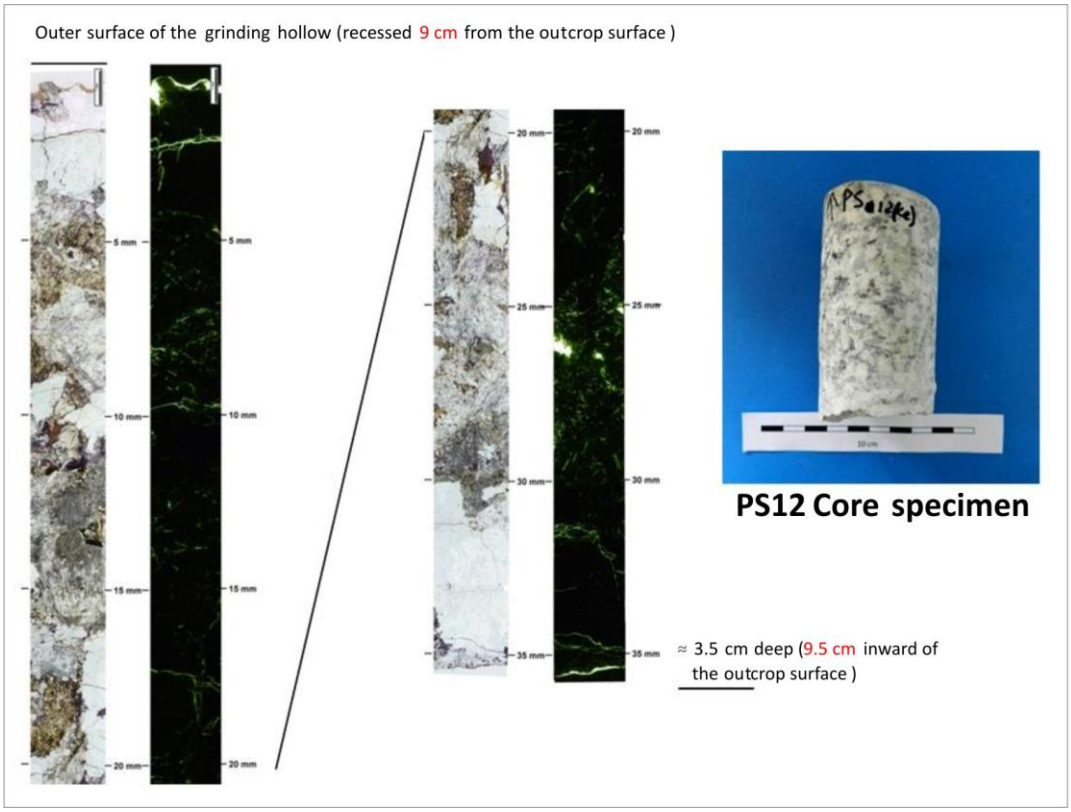

Figure 10. Vertical thin section of core sample PS 12 (Pozo Serafín): left column, polarised light micrograph; right, fluorescent light micrograph, in which cracks and pores are more readily visible (each vertical section is a mosaic of 22 microphotographs).

In the granodiorite (outcrops PS and ST), however, the cracks were mostly associated with weathered feldspar and mica-rich areas (Figure 10). These samples also exhibited intracrystal cracks, which were rare in the monzogranite. The micas in the granodiorite were observed to be arranged in layers. At the Pozo Serafín outcrop, such layering was even visible at the corners of the BRMs (Figure 11).

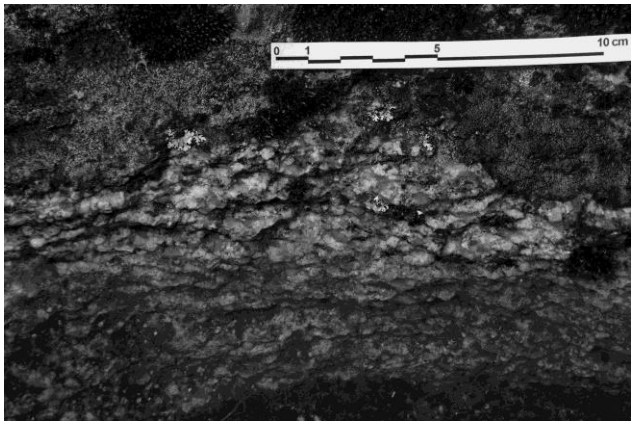

Figure 11. Layered mica in granodiorite stone

The mercury intrusion porosimetry findings (Table I and figure 12) showed that microporosity rose with depth (difference between the samples from the area outside the BRMs (AOBRM) and the specimens cored at the centre of the BRMs), while macroporosity declined. Pore size distribution also differed in the monzogranite (median pore size range, 0.1-1 µm) and the granodiorite (median pore size range, 1-10 µm for RB (AOBRM) and two medians for RB-4, 0.1-1 and 1-10 µm) stone.

Table I. Mercury intrusion porosimetry for a sampling of core specimens

Sample ID	Total porosity	Micro < 5 µm	Macro > 5 µm
PS (AOBRM)	1.4%	73.2%	26.8%
PS-12	1.8%	78.1%	21.9%
ST (AOBRM)	1.4%	75,6%	24,4%
ST-4	2.1%	80.8%	19.2%
RB (AOBRM)	2.7%	63.5%	36.5%
RB-4	1.9%	83.3%	16.7%

PS: Pozo Serafín, ST: Sierpe Tres, RP: Ribera del Pontón, AOBRM: area outside BRM.

These differences in characteristics also explain the dissimilar behaviour in the ultrasound velocity observed for the two types of rock. Mineral and textural distribution affected the rock anisotropy calculated from Vp. At the Pozo Serafín outcrop, material anisotropy was found to vary from 29 to 23 between depths of 10 to 15 cm (Vázquez-Calvo et al., 2013), values that concurred with the mean depth of the BRMs (Table II). Similar findings were observed at

the Ribera del Pontón outcrop, where anisotropy declined from 22 to 14 at a depth of around 8 cm, likewise concurring with the mean depth of the BRMs in this outcrop (Table II).

At Sierpe Tres, however, a change (from 39 to 31) was recorded in anisotropy at around 5 cm, concurring with the depth of three of the BRMs but not the the other two (Table II). Moreover, the anisotropy values (39-31) were higher there than observed in the Pozo Serafín outcrop. While changes in anisotropy may have affected the depth reached in each BRM, other parameters such as hardness may have also played a significant role.

Table II. Mean ultrasound velocity and hardness index values for selected BRMs

BRM	Vp (m/s)	Hardness index	Maximum BRM depth (cm)
ST			
ST-3	2043±648	40±12	10
ST-4	1637±383	42±12	4
ST-6	1834±682	33±8	3
ST-24	2970±1126	48±12	7
ST-25	1422±332	41±8	10
PS			
PS-8	1977±858	41±13	18.5
PS-12	1863±845	44±16	9
PS-23	1305±212	35±8	10.5
RB			
RB-3	1340±295	44±11	8
RB-4	1557±374	45±17	9
RB-5	1609±463	46±12	8
RB-9	2050±385	38±12	9
RB-10	1596±239	36±6	6.5
RB-11	1600±621	33±6	8

PS: Pozo Serafín, ST: Sierpe Tres, RP: Ribera del Pontón,

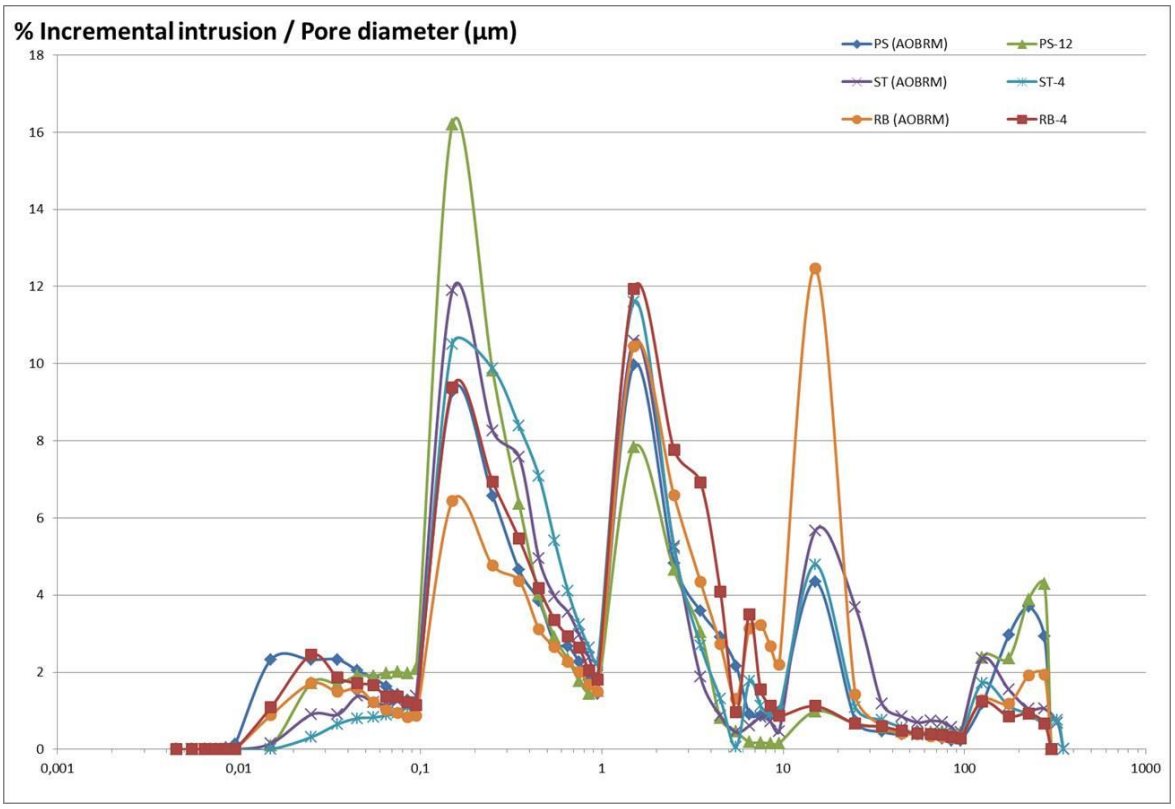

Figure 12. Mercury intrusion porosimetry for a sample of core specimens: PS, Pozo Serafín; ST, Sierpe Tres; RP, Ribera del Pontón; AOBRM, area outside BRM (pore dimeter represented on a logarithmic scale).

On the grounds of the foregoing, both the mean ultrasound velocity and the mean hardness index for each BRM (Table II) would appear to deliver useful information for determining the stage of its usability. The mean hardness index inside these depressions was found to be ≈40 and the mean ultrasound velocity to be ≈1700 m/s. It might consequently be thought that surfaces with hardness values of over 40 or ultrasound velocities of under 1700 m/s would no longer be usable. Nonetheless, not all the BRMs followed that pattern. Consequently, the most suitable method for establishing their usability is to plot the mean hardness index versus the mean ultrasound velocity, as these two parameters established the differences both quantitatively and fairly clearly (Figure 13).

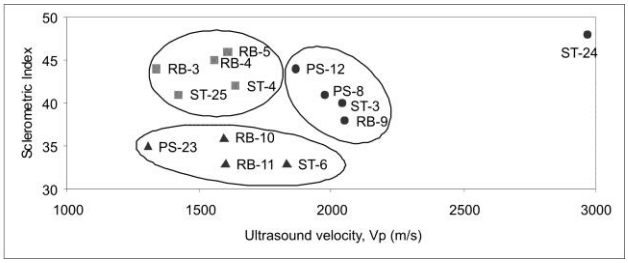

Figure 13. Mean hardness index versus mean ultrasound velocity for selected BRMs

Three groups can be identified from the plots in Figure 13. One would comprise the BRMs that were no longer usable (shown as solid dots:, PS-8, PS-12, ST-3 and RB-9). ST-24, while clearly an outlier due to the high values observed, was likewise unusable. The BRMs in the group of outcrops represented by triangles (PS-23, ST-6, RB-10, RB-11) were still usable. The remaining mortars (represented by squares) may or may not have still been usable, because while their ultrasound velocity was low their hardness index was high. These findings can be also correlated to the hardness profiles plotted in Figure 7. Most of the BRMs in Figure 8 with uncertain usability (RB-3, RB-4, RB-5 and ST-25) had profiles similar to the ST-25 profile in Figure 8, while the ST-4 profile was much like the PS-12 profile in Figure 8. The inference might be that BRMs with profiles of these characteristics and hardness values mostly over 40 were no longer usable. Further to that reasoning, those with low ultrasound velocity values but high hardness indices might be regarded as unusable.

Roughness measurements were taken at the corners and centres of the BRMs, as shown in Figures 14a and b. Roughness was greater at the corners, as would be expected, for rubbing would have been more intense in the deeper areas. Parameter Rz was used to compare the BRMs. The Rz values were found by summing the vertical distances between the five highest peaks and five deepest valleys on 25 mm2 micro-topographic maps. These measurements were taken at the centre of the BRMs, however, to prevent the rock anisotropy visible at the corners of the Pozo Serafín BRMs (Figure 15) from distorting the results. The mean Rz values are listed in Table III.

Table III. Mean Rz at the centre of BRMs

Outcrop	Rz
Pozo Serafín	26.7
Sierpe Tres	26.4
Ribera del Pontón	31.1

The means for the Pozo Serafín and Sierpe Tres BRMs were similar and smaller than the Ribera del Pontón measurements. Those findings infer that the type of granite had a greater impact on Rz than the depth of the BRM (and therefore than the length of time that the surface was used or the working method deployed). The grooves occasioned by grinding were unfortunately too large (Figure 16) to be studied with a 3D optical roughness meter, although roughness, in terms of the roughness meter scale, was clearly observed to intensify in readings C2, C3 and C4 of the mortar stone (Figure 14a).

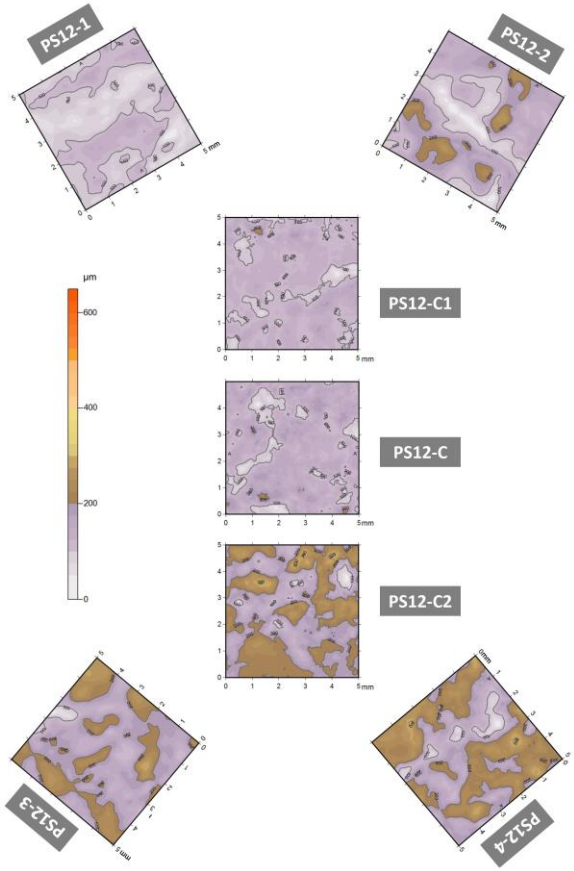

Figure 14a. Two-dimensional roughness maps for Pozo Serafín BRM PS12: C= centre of BRM; 1-4 = the corners; C1-C2, maps of areas above and below the centre, respectively

7. CONCLUSIONS

A number of petrological techniques were used to characterise BRMs (depressions formed by gold ore grinding) in granite outcrops around the Pino del Oro gold mines. The evidence found suggested that changes in anisotropy may be related to the depth of these bedrock mortars. In addition, a comparison of the characteristics of the two kinds of granites bearing these depressions and the findings for the various techniques showed that the approach best suited to the present purposes was the elaborate/ interpret together the hardness index and ultrasound velocity.

Such assessments inter-related physical characteristics of the BRMs such as density, compactness, porosity and hardness, which are relatively easy to measure empirically. Based on these findings, a hypothesis was put forward to the effect that Vp velocities of over 1700 m/s would be an indication that the works had reached a final stage, while lower velocities stand as evidence of works in an initial stage or in progress.

Nonetheless, high hardness indices (over 40), would denote final stage works even in the presence of low ultrasound velocities. Nonetheless, high hardness indices (over 40), would denote final stage works even in the presence of low ultrasound velocities. Assuming that hypothesis to be correct, the three outcrops were still usable when they were abandoned. Further work is required in this respect, for measuring all the BRMs in all the outcrops (over 1000 have been identified in about 60 outcrops) and applying the working hypothesis might provide grounds for determining how work was distributed in each outcrop, or even for identifying outcrops with no usable BRMs. As mentioned in the objective, ore-related research is also underway.

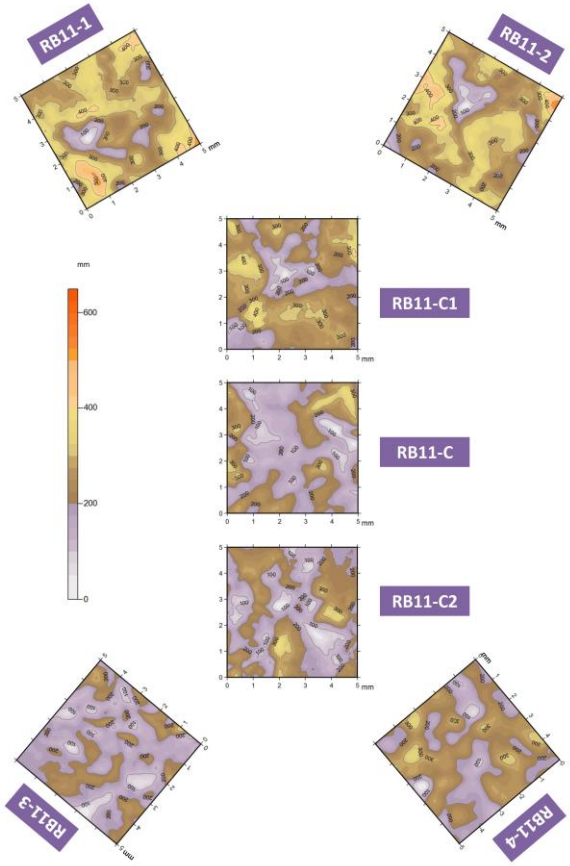

Figure 14b. Two-dimensional roughness maps for Ribera del Portón BRM RB12: C = centre of BRM; 1-4 = the corners; C1-C2, maps of areas above and below the centre, respectively

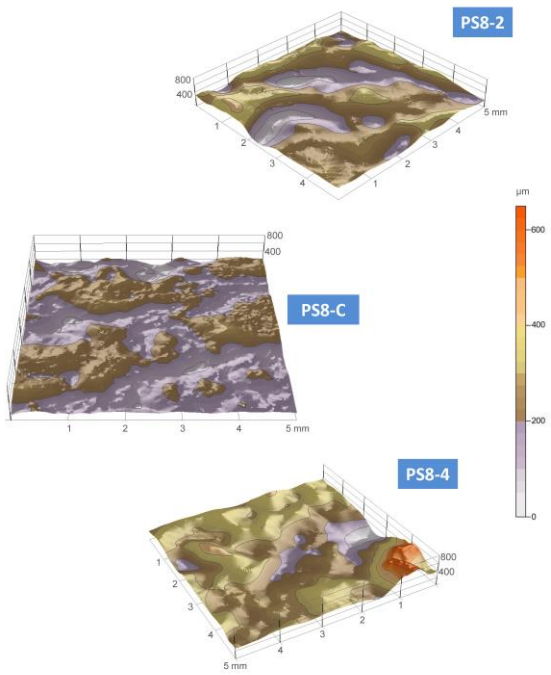

Figure 15. Three-dimensional roughness maps for Pozo Serafín BRM PS8: C = centre of BRM; 2 and 4, top and bottom right corners, whose curved grooves reflect rock anisotropy

Preliminary findings show, for instance, that the hardness of the quartz fragments characteristic of the ore are similar to the hardness of BRMs here regarded as still usable. If such information can be gathered, it may be possible to establish whether the proximity of a quartz vein or other factors influenced the choice of mining sites.

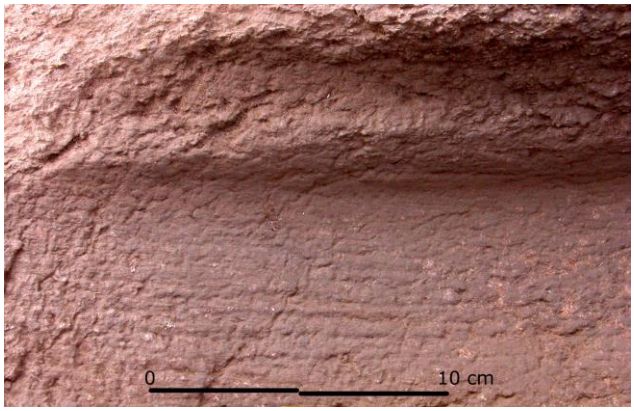

Figure 16. Grooves occasioned by grinding

ACKNOWLEDGEMENTS

This research was funded under the Consolider-Ingenio 2007 (CSD2007-0058), "Paisajes de dominación y resistencia. Procesos de apropiación y control social y territorial en el noroeste hispano" (HAR2012-33774) and Geomateriales 2 (S2013/MIT_2914) programmes. The authors wish to thank Valle López for helping to chart the roughness maps and Ana Delia Rodríguez and Juan Luis Pecharromán for their assistance with the field work.

REFERENCES

Burnham, B. & Burnham H. (2004). Dolaucothi-Pumsaint. Survey and excavations at a Roman Gold-Mining complex 1987-1999. University of Wales, Oxbow Books, Oxford.

Fort, R., Varas, M.J., Alvarez de Buergo, M. and Freire, D.M. (2011). Determination of anisotropy to enhance the durability of natural stone. *Journal of Geophysics Engineering*. Vol. 8, 132-144.

Fort, R., Vazquez-Calvo, C., Chapa, T., Martínez-Navarrete, M.I. and Belén, M. (2013a). Analytical study of Iberian Iron Age stone sculptures and their surface marks. *Archaeometry*, Vol. 55 (3), 391-406.

Fort, R., Alvarez de Buergo, M. and Perez-Monserrat, E. (2013b). Non-destructive testing for the assessment of granite decay in heritage structures compared to quarry stone. *International Journal of Rock Mechanics and Mining Sciences*, Vol. 61, 296-305.

González-Clavijo, E., Álvarez, F. and Diez Balda, M. A. (1991). La cizalla de Villalcampo (Zamora) geometría cinemática y condiciones de la deformación asociada. *Cadernos do Laboratorio Xeolóxico de Laxe*, Vol. 16, 203-219.

Goudie AS. (2006). The Schmidt Hammer in geomorphological research. *Progress in Physical Geography*, Vol. 30, 703–18.

Jiménez Benayas, S. Crespo Ramón. J. L., Cabrera Ceñal, R., García de los Ríos Cobo, J. I., Mediavilla Manzanal, B. and Armenteros Armenteros, I. (1997). Mapa Geológico y Minero de Castilla y León. 1:400.000. Sociedad de Investigación y Explotación Minera de Castilla y León, S.A. (SIEMCALSA).

Onishi, C.T. and Shimizu, I. (2005). Visualization of microcrack anisotropy in granite affected by a fault zone, using confocal laser scanning microscope. *Journal of Structural Geololgy*, Vol. 27 (12), 2268-2280.

Quiroga de la Vega, J., Sánchez Cela, V., Gabaldón López, V., León Gómez, C. and Solar Menéndez, J.B., (1981). Hoja geológica 1:50.000 nº 367, Castro de Alcañices. 2ª Serie-1ª edición, Instituto Geológico y Minero de España (IGME), Madrid.

Quiroga de la Vega, J., Sánchez Cela, V., Gabaldón López, V., León Gómez, C., Quinquer Augut, R. and Solar Menéndez, J.B. 1982. Hoja geológica 1:50.000 nº 368, Carbajales de Alba. 2ª Serie-1ª edición, Instituto Geológico y Minero de España (IGME), Madrid.

RILEM (Ed). (1980). Recommended tests to measure the deterioration of stone and to assess the effectiveness of treatment methods. *Materials and Structures*. Vol. 75, 175-253.

Sánchez-Palencia, F. J, Sastre Prats, I., Romero Perona, D., Beltrán Ortega, A., Pecharromán Fuente, J. L., Alonso Burgos, F., Currás Refojos, B. X. and Reher Díez, G. S. (2010ª) La zona minera de Pino del Oro (Zamora), un paisaje rural de época romana In Fornis, C. , Gallego, J., López Barja de Quiroga, P. M. (Coords.) *Dialéctica histórica y compromiso social. Homenaje a Domingo Plácido*. Vol. 2. (pp . 1067-090) Portico, Zaragoza,

Sánchez-Palencia, F. J., Beltrán, A., Romero, D., Alonso, F. and Currás, B. (2010b). *La zona minera de Pino del Oro (Zamora)*. Guía arqueológica. Junta de Castilla y León, Valladolid.

Sánchez-Palencia, F. J. and Currás Refojos, B. (2010). El contexto geoarqueológico: la zona minera de Pino del Oro. *El bronce de El Picón (Pino del Oro). Procesos de cambio en el occidente de Hispania.* (pp. 15-38) .Junta de Castilla y León, Valladolid,

Vázquez-Calvo, C., Varas, M.J., Álvarez de Buergo, M. and Fort, R.(2010). Limestone on the "Don Pedro I" facade in the Real Alcázar compound, Seville, Spain. *Limestone in the Built Environment: Present Day Challenges for the Preservation of the Past.* Geological Society Special Publication - The Geological Society of London, (Vol. 331, pp 171–182) Geological Society Publishing House, Bath.

Vázquez-Calvo, C., Alvarez de Buergo, M., Fort, R., and Varas-Muriel M.J. (2012). The measurement of surface roughness to determine the suitability of different methods for stone cleaning. *Journal of Geophysics Engenieering*. Vol. 9, 108-117.

Vázquez-Calvo, C., Fort, R., Romero, D., Beltrán, A. and Sánchez-Palencia, F-J. (2013) A petrological approach to the study of grinding mortars from the Roman gold mines of "Pino del Oro" (Zamora, Spain). *Science and Technology for the Conservation of Cultural Heritage* (pp 353-356) CRC Press, Taylor and Francis Group.